Integrative Biology

PAPER

View Article Online
View Journal | View Issue

Cite this: *Integr. Biol.*, 2014, **6**, 1132

The potential of microfluidic lung epithelial wounding: towards *in vivo*-like alveolar microinjuries†

M. Felder,[ab] A. O. Stucki,[ab] J. D. Stucki,[ab] T. Geiser[cd] and O. T. Guenat*[ace]

Received 27th June 2014,
Accepted 2nd September 2014

DOI: 10.1039/c4ib00149d

www.rsc.org/ibiology

Idiopathic pulmonary fibrosis (IPF) remains a major clinical challenge to date. Repeated alveolar epithelial microinjuries are considered as the starting point and the key event in both the development and the progression of IPF. Various pro-fibrotic agents have been identified and shown to cause alveolar damage. In IPF, however, no leading cause of alveolar epithelial microinjuries can be identified and the exact etiology remains elusive. New results from epidemiologic studies suggest a causal relation between IPF and frequent episodes of gastric refluxes resulting in gastric microaspirations into the lung. The effect of gastric contents on the alveolar epithelium has not been investigated in detail. Here, we present a microfluidic lung epithelial wounding system that allows for the selective exposure of alveolar epithelial cells to gastric contents. The system is revealed to be robust and highly reproducible. The thereby created epithelial microwounds are of tiny dimensions and best possibly reproduce alveolar damage in the lung. We further demonstrate that exposure to gastric contents, namely hydrochloric acid (HCl) and pepsin, directly damages the alveolar epithelium. Together, this novel *in vitro* wounding system allows for the creation of *in vivo*-like alveolar microinjuries with the potential to study lung injury and alveolar wound repair *in vitro*.

Insight, innovation, integration

Current *in vitro* wounding systems are limited in reproducibility and often fail to mimic injuries of smallest dimensions, as observed in the epithelium of the human alveolus. Here, we present a microfluidic wounding system that allows for the formation of tailor-made *in vivo*-like alveolar microinjuries. With the aid of an aqueous two phase system, we demonstrate that exposure to gastric contents causes alveolar injuries with profound loss of epithelial barrier integrity, a key event in the development of pulmonary fibrosis. Such wounding systems for injuries with dimensions relevant to the human alveolus may crucially contribute to a better understanding of the pathomechanisms underlying chronic lung diseases.

Introduction

Idiopathic pulmonary fibrosis (IPF) is a chronic, progressive and fatal lung disease of unknown origin. Initially, IPF was thought to be the consequence of chronic low-grade inflammation in the lung parenchyma. However, during the past few decades anti-inflammatory treatment strategies were revealed to be ineffective in IPF patients. Furthermore, new results suggest that fibrosis evolves even in the absence of inflammation. These findings led to a clear distinction between fibrotic and inflammatory processes,[1] followed by a paradigm shift in the pathomechanism underlying IPF. Consequently, a "deregulated alveolar repair" model replaced the prevailing hypothesis of "inflammation-driven" IPF.[2,3] Accordingly, pulmonary fibrosis is the consequence of improper wound healing upon repeated injuries to the alveolar epithelium. In a healthy lung, the alveolar epithelium regenerates after injury by the action of type II alveolar epithelial cells. These cells act as local progenitor cells of the alveolus and show stem cell-like properties.[4,5] In IPF, however, the self-regenerative potential of the alveolus is overstrained and the injured epithelium is replaced by non-functional restrictive scar tissue. Injuries to the alveolar epithelium are typically of tiny dimensions ranging from

[a] *ARTORG Center Lung Regeneration Technologies Lab, University of Bern, Murtenstrasse 50, 3010 Bern, Switzerland. E-mail: olivier.guenat@artorg.unibe.ch*
[b] *Graduate School for Cellular and Biomedical Sciences, University of Bern, Freiestrasse 1, 3012 Bern, Switzerland*
[c] *Division of Pulmonary Medicine, University Hospital of Bern, Freiburgstrasse 4, 3010 Bern, Switzerland*
[d] *Department of Clinical Research, University of Bern, Murtenstrasse 50, 3010 Bern, Switzerland*
[e] *Division of Thoracic Surgery, University of Bern, Feiburgstrasse 4, 3010 Bern, Switzerland*

† Electronic supplementary information (ESI) available. See DOI: 10.1039/c4ib00149d

single cell death to multicellular lesions, hereinafter referred to as alveolar microinjuries. Numerous pro-fibrotic agents with deleterious effects on alveolar epithelial cells were identified. Among those, microaspirations of gastric refluxates recently emerged as potential key factors in the development of IPF.[6,7] Indeed, epidemiologic studies revealed a significantly higher prevalence of gastroesophageal reflux disease (GERD) among IPF patients (66–94% *vs.* 10–20% in control population).[8–10]

Microaspirations are episodes of gastric reflux inhalations that enter into the peripheral lung. Such refluxates can be gaseous, liquid or a mixture of both with various acidic concentrations.[11] The detection of pepsin, a digestive enzyme from the stomach, in bronchoalveolar lavage (BAL) fluid has become an unequivocal marker for microaspirations.[12,13] Similar to other digestive enzymes, pepsin is secreted as an inactive pro-enzyme and activated only upon its proteolytic cleavage at the site of action. The activation of pepsin is strongly pH-dependent and triggered by hydrochloric acid (HCl). Peak activity of pepsin was reported at pH 1.5–2.5,[14] which correlates with normal HCl-levels in gastric juice. Peptic activity gradually decreases with increasing pH-levels with complete inactivation at neutral pH. In the pH-range of acidic microaspiration (pH < 4), however, approximately 70% of the peptic peak activity persists. Interestingly, Johnston and colleagues demonstrated that inactive pepsin at neutral pH remains stable on laryngeal epithelium after a simulated reflux event.[15] Subsequent pH-drops, possibly induced by successive acidic microaspirations, can then reactivate the silenced pepsin and cause severe tissue damage. Similar studies report pepsin-induced cell injuries in esophageal[16] and bronchial cells.[17] However, the effect of pepsin on peripheral lung epithelium and its potential implications for the development of IPF remain unknown.

In this study, we present an *in vitro* microfluidic wounding model that allows for the reproduction of *in vivo*-like alveolar epithelial microinjuries. In the first step, epithelial wounds of dimensions relevant to the human alveolus,[18] are reproduced. Therefore, a trypsin–EDTA based flow focusing technique reported recently by our group and others for epithelial[19] and endothelial[20] wound healing is pushed to its limit to inflict microinjuries of smallest wound dimensions. In sharp contrast to conventional scratch assays, this technique allows targeting a very limited amount of cells and enables the formation of micrometer-wide epithelial injuries. Such microinjuries are thought to be the trigger and the cause of progression in IPF. An adequate *in vitro* reproduction of the alveolar microinjuries is therefore crucial for the investigation of IPF-related alveolar wound healing. In addition, a multiple of those injuries are created within the same epithelial layer to modulate multi-focal lesions, typically found in IPF. In the second step, an *in vivo*-like wounding agent is investigated. Although, trypsin-induced lung injury has been demonstrated in a rat model of pancreatitis,[21] its physiologic relevance in humans remains limited.[22] Therefore, instead of trypsin, two key compounds of gastric refluxates, pepsin and hydrochloric acid (HCl), were used to induce microinjuries to the alveolar epithelium. The presence of a strong acid in the flow focusing system leads to an additional difficulty, the fast diffusion of protons across the microfluidic system. To overcome this limitation, an aqueous two-phase system is implemented to limit the diffusion of protons and to allow the acidified pepsin solution to remain active in the central flow. Aqueous two-phase systems have recently been reported in the context of cell culture in a microfluidic environment. Takayama and colleagues described a patterning technique for selective cell and reagent deposition,[23,24] whereas Petrak *et al.* microprinted cells to create organized constructs for tissue engineering applications.[25] The aqueous two-phase technique is used here for the first time to create flow focused microwounds in a confluent cell layer. The resulting microwounds unprecedentedly recapitulate microaspiration-induced lung injuries.

Materials and methods

Microfluidic platform: design and fabrication

A system of converging microchannels was designed using CAD-based construction software to enable hydrodynamic flow focusing. The design (Fig. 1) consists of a 750 μm wide and 10 mm long rectangular microchannel that can individually be accessed on each side by three separate inlets and outlets, respectively. Inlets and outlets, hereinafter referred to as access channels, are 210 μm wide and 4.5 mm long. The 100 μm high microfluidic channel has a total volume of 0.75 μl, whereas the access channels each have a volume of roughly 0.1 μl. An epoxy mold, made of Accura Extreme, was fabricated by stereolithography (Proform AG, Switzerland). Soft replicas of polydimethylsiloxane (PDMS, Dow Corning) casts were manufactured according to standard rapid prototyping protocols(24). Access ports were punched using a 1.5 mm dermal biopsy punch (Shoney Scientific, India). PDMS casts and microscope glass slides were then sonicated for 5 min in 100% ethanol (EtOH), rinsed with purified water and

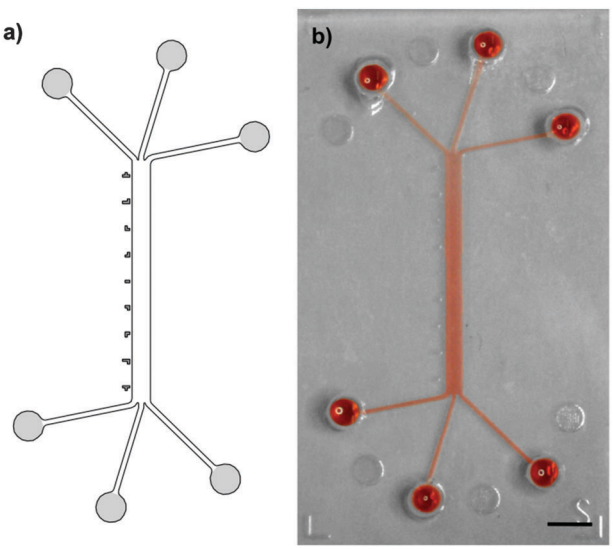

Fig. 1 Schematic drawing (a) and picture (b) of the microfluidic platform filled with red dye. Six regularly arranged access channels converge into a 750 μm wide, 100 μm high and 10 mm long rectangular microchannel. Six identical access ports (highlighted in light gray), mark the entry to the three individual inlets or outlets, respectively. Nine unambiguous position markers (highlighted in dark gray) are evenly distributed along the microchannel. Scale bar: 2 mm.

dried with compressed air. Exposure to O_2-plasma for 25 s at 650 mTorr (Harrick Plasma, USA) enabled covalent bonding of PDMS casts and glass slides. After bonding, the assembled microfluidic platforms were post-baked overnight at 60 °C in order to strengthen the sealing between the PDMS cast and the glass substrate.[26]

Epithelial cell culture

Cell culture experiments were performed according to a protocol described previously.[19] In brief, all cell manipulations were performed under a laminar flow cabinet according to aseptic working techniques. Human type II alveolar epithelial-like A549 cells (ATCC, USA), passage numbers 20 to 40, were cultured in RPMI 1640 medium (Gibco) supplemented with 10% fetal bovine serum (Gibco), 100 U ml^{-1} penicillin and 100 μg ml^{-1} streptomycin (Gibco), hereinafter referred to as complete culture medium. Microfluidic platforms, prior to experimentation, were sterilized using UV-exposure for 15 min and rigorous rinsing with 70% ethanol (EtOH). Sterilized platforms were then wetted with isopropanol, followed by serial dilutions of EtOH, sterile water and complete culture medium. The four lateral access ports were plugged with autoclaved and hermetically sealed polyether ether ketone (PEEK) tubings of approximately 1.6 mm (1/16″) outer diameter (VWR). Overnight incubation of complete culture medium at 37 °C and 5% CO_2 in the microfluidic platform enabled protein adsorption to the PDMS cast[27] and basic coating of the glass substrate. High density cell suspension of 6×10^6 cells per ml was then injected into the central inlet port resulting in a seeding density of 6×10^3 cells per cm^2. Excess medium was removed. Loaded microfluidic platforms were then placed in humidity chambers and incubated at 37 °C and 5% CO_2. Once the epithelial cells firmly adhered to the substrate, the central inlet port was connected to a medium filled syringe (BD Biosciences, USA) using 1.6 mm diameter Polytetrafluoroethylene (PTFE) tubings (Bohlender, Germany). Medium filled syringe reservoirs were further loaded on respective syringe pumps (Harvard Apparatus, USA). Under continuous perfusion with 0.1 μl min^{-1} complete culture medium, cells were grown to confluence within two to three days. The displaced medium was collected in 1.5 ml eppendorf tubes *via* PTFE tubings. Upon confluence, the entire microchannel system was rinsed twice with pre-warmed (37 °C) complete culture medium.

Trypsin–EDTA epithelial layer wounding

Hydrodynamic flow focusing was used to expose a confluent layer of alveolar epithelial-like (A549) cells to tailored wounding patterns as reported earlier.[19] Briefly, a central flow carrying a wounding agent, 0.5% trypsin–EDTA (Gibco), was maintained in the middle part of the channel while complete culture medium was perfused on both sides of the main flow stream. These sheath flows protected the underlying epithelial layer. Three independent parameters (the microwound width, the time to create a microinjury in the cell layer and the microwound localization) were investigated to fully explore and evaluate the potential of microfluidic wound creation based on flow focusing. The corresponding experimental set-ups are described in detail below. Importantly, in order to provide uniform culture conditions, all wounding experiments were performed under a predefined level of shear stress by utilizing a constant overall flow rate of 15 μl min^{-1}.

Microwound width. Complete culture medium and the trypsin–EDTA solution were injected from two syringe pumps. Prior to experimentation, the sheath flows were each injected at 7.5 μl min^{-1} for 5 min. Trypsin–EDTA was then injected at a flow rate of 0.5, 1, 2, 3 and ultimately 5 μl min^{-1}, while, at the same time, the sheath flow was reduced accordingly to maintain an overall flow rate of 15 μl min^{-1}. The ratio between the wounding and the overall flow rate was thereby set at 1 : 30, 1 : 15, 1 : 7.5, 1 : 5 or 1 : 3, respectively. Between each consecutive wounding episode, the wounding flow was transiently stopped and the cells were washed for 3 min with complete culture medium only. Bright-field micrographs were taken using the JuLI Fluorescent Cell Analyzer (Witec, Switzerland) before and after each wounding at 10 succeeding channel segments along the entire microchannel. Using FIJI software (NIH, USA), the wound width was then measured at 5 random positions within every channel segment. Data derived from channel segments with apparent flow disturbances, such as cell aggregates, dust particles or air bubbles, were excluded from further analysis. Similarly, segments in proximity to the channel openings were excluded from analysis. Thereby, only data from undisturbed and fully developed parabolic flow profiles were utilized. Data are represented as means ± standard deviations of four independent experiments.

For visualization purposes, sodium-fluorescein (F6377, Sigma) was dissolved in D-PBS (Gibco) to a final concentration of 1 mg ml^{-1} and injected together with the sheath flow of D-PBS only into a microfluidic platform without cells. Bright-field and fluorescence micrographs were taken at the corresponding segments and overlaid using digital image processing software (AxioVision, Zeiss). To determine the theoretical wound widths, a simple computer simulation was run using the finite-element analysis software COMSOL Multiphysics. The laminar flow simulation is based on the Navier–Stokes equation with no slip boundary conditions (velocity at the border is zero). Streamline projections from the central inlet were plotted for the five indicated flow ratios 1 : 3–1 : 30. The theoretical wound widths were then determined by the resulting width of the streamline projections in the center of the channel.

Time to create a microinjury in the epithelial layer. The microfluidic platform was mounted on a stage top incubator of a Zeiss LSM710 laser scanning microscope equipped with an automated stage drive for live cell imaging at 37 °C and 5% CO_2. Both trypsin–EDTA and complete culture medium were perfused *via* long PTFE-tubing arranged within the incubation box to adjust for temperature variations. A centered flow of focused trypsin–EDTA was then injected for selective cell exposure. Similar to the aforementioned wound width analysis, five different exposure patterns were tested: 1 : 30, 1 : 15, 1 : 7.5, 1 : 5 and 1 : 3. A fully confluent cell layer was used for every exposure pattern. Wound formation was monitored by a series of consecutive micrographs recorded along the entire microchannel length. This procedure was repeated every other minute during the

whole experiment. Consecutive micrographs were then stitched together using the MosaicJ plugin of the FIJI software. At each time point, the length of the created wound was determined as the distance between the channel opening and the position at which the most distant cell detached.

Microwound localization. To precisely control the localization of the focused flow of trypsin–EDTA within the microchannel, the sheath flow was injected *via* two separate syringe pumps. In Fig. 5, a representative example of this set of experiments is depicted. Trypsin–EDTA was injected at 2 μl min^{-1} into the central inlet. Meanwhile, complete culture medium was perfused at a total of 13 μl min^{-1} (ratio central-to-sheath flow 1 : 7.5) from the lateral inlets. In contrast to the aforementioned experiments, complete culture medium was injected at unequal flow rates from the lateral inlets. In the first step, the sheath flow was injected at 3 μl min^{-1} from the left and 10 μl min^{-1} from the right inlet. The focused flow of trypsin–EDTA was thus directed towards the left. After formation of a first de-centered microwound, the sheath flow injection mode was reversed to 10 μl min^{-1} from the left and 3 μl min^{-1} from the right. Consequently, the focused flow of trypsin–EDTA was re-directed towards the right. Micrographs were taken before and after each wounding.

Pepsin–HCl epithelial layer wounding

To mimic microaspirations during episodes of gastric refluxes, we developed a novel wounding agent based on two key components of gastric refluxates, pepsin (Sigma-Aldrich) and hydrochloric acid (HCl, Merck). To reduce diffusion-related artefacts, we established an aqueous two-phase system (Fig. S3, ESI†), based on the study reported by Frampton *et al.*,[23] aimed at cell co-culture patterning. 5% (w/w) high molecular weight dextran (DEX 500 kDa, Pharmacosmos, Denmark) and 2.5% (w/w) low molecular weight polyethylene glycol (PEG 35 kDa, Fluka) were added to serum-free cell culture medium. Polymers were then completely dissolved overnight using a rotator (Intelli-Mixer RM-2, ELMI Ltd, Latvia), followed by centrifugation at 1000*g* for 15 min to accelerate phase separation. Once the phases were fully separated, both the PEG-rich upper and the DEX-rich lower phase appeared clear with a sharp separation line at their interface. The lower phase was then isolated and subsequently used as sheath flow. The upper phase, in contrast, was acidified with HCl to pH 4. Then, pepsin was added to reach a final concentration of 2.5 mg ml^{-1}. Acidification processes were monitored using a pH-meter (SevenEasy, Mettler Toledo). If needed, the pH was readjusted after pepsin dissolution by fine titration using diluted HCl and sodium hydroxide (NaOH, Sigma). Prior to their use, both solutions, the DEX-rich lower phase and the acidified and pepsin-supplemented PEG-rich upper phase, were then filtered through 0.2 μm pored polyethersulfon syringe filters (VWR) for sterilization.

Similar to the time to create the microwound analysis, the microfluidic platform was mounted on the stage-top incubator of the Zeiss LSM710. The acidified and pepsin-supplemented wounding agent was then perfused at a 1 : 15 ratio with respect to the pH-neutral DEX-phase. Micrographs of succeeding channel segments along the entire microchannel were taken every other minute to monitor the wound formation.

Results and discussion

Lung epithelial cells (A549) were cultured to confluence in a microfluidic environment prior to being wounded. These cells form a functional monolayer of type II alveolar epithelial cells in such a perfused environment, as previously demonstrated by immunostaining and transmission electron micrographs.[19] Type II alveolar epithelial cells have self-renewal capacity and were shown to be mainly responsible for epithelial regeneration upon alveolar injury. Such systems have therefore been used to investigate alveolar wound healing *in vitro*.[28,29] While the cells were cultured at a low flow rate of 0.1 μl min^{-1} during the growth phase, the flow conditions during the wounding phase took place at an elevated flow rate of 15 μl min^{-1}, which corresponds to a Reynolds number of 1.5 and to a shear stress of about 1.5 dyne per cm^2. This level of shear stress is well within the physiologic range of 0.5–3 dyne per cm^2 reported during normal breathing.[30] Although this shear stress is rather small, it should be emphasized that mechanical stretch and shear stress are considered to be crucial factors in the development of epithelial microwounds in the lung.[31–34] Particularly, during acute exacerbations, the mechanical load on the epithelial cells may increase disproportionately. A causal link between acute exacerbations in IPF and occult microaspirations has recently been postulated.[35]

To explore the versatility and the potential associated with this wounding system, the alveolar epithelial cells were exposed to various wounding patterns. The experimental procedure was revealed to be very robust and reproducible. This high reproducibility is attributed to the laminar flow conditions present in the microfluidic system.

Trypsin–EDTA-induced injury: control of the wound width

It is the objective of this study to create microinjuries of smallest possible dimensions, as they appear *in vivo* at the cellular level within the alveolar sacs. Hydrodynamic focusing was used to selectively expose a confluent layer of alveolar epithelial cells to a series of different flow conditions. Trypsin–EDTA was used as the cell dissociation agent. Thereby, EDTA effectively chelates divalent Mg^{2+} and Ca^{2+}-ions from calcium-dependent cell adhesion molecules (cadherins) and integrins. Similarly, trypsin proteolytically cleaves cell anchoring and adhesion molecules, such as integrins and cadherins. Consequently, cells exposed to the focused flow of trypsin–EDTA were dissociated from the intact cell layer and released from the substrate. Fig. 2 illustrates the resulting microwounds in the alveolar epithelium obtained for the five flow conditions examined. Wound widths were measured and are summarized in Fig. 3. The standard deviations among all flow conditions were found to be 10–16 μm, which correlates with the size of a single A549 cell[36] and is an excellent indicator of the robustness and reproducibility of the technique. For the formation of the smallest microwounds (flow ratio 1 : 30), trypsin–EDTA was injected at 0.5 μl min^{-1}, while complete culture medium was perfused at 7.25 μl min^{-1} in the lateral inlets, resulting in a cell-free area of only 42 μm in width. The size of the microwounds corresponded very well with the area exposed to trypsin–EDTA,

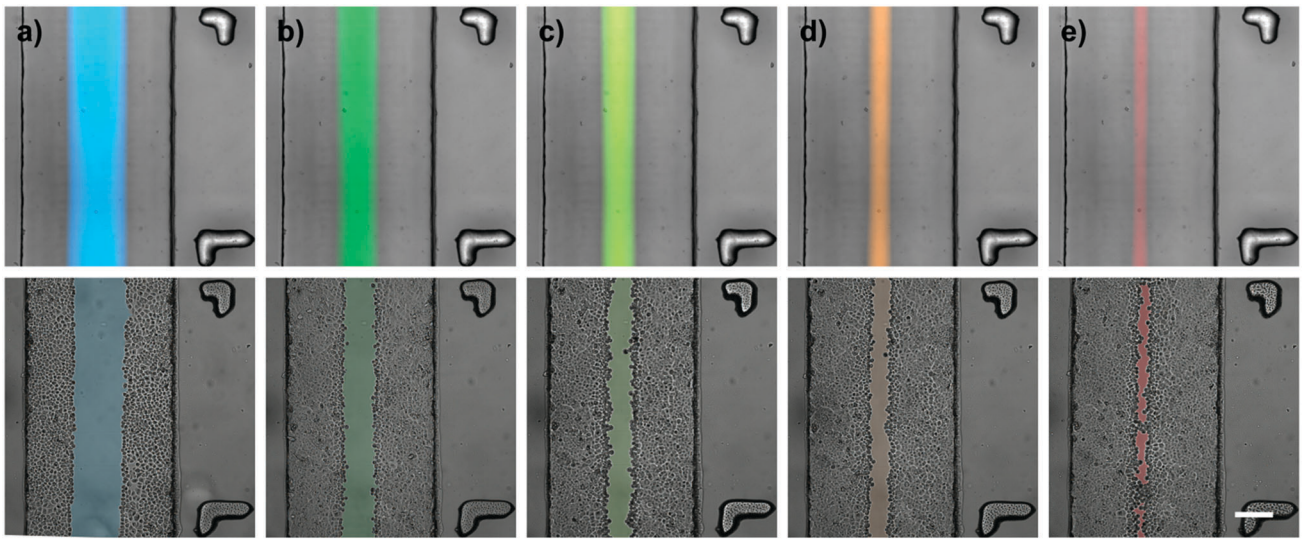

Fig. 2 Representative micrographs of hydrodynamic flow focusing in a 750 μm wide microchannel. Top line: pseudo-colored sodium fluorescein bound by D-PBS; Bottom line: confluent A549 cells exposed to 0.5% trypsin–EDTA sheathed by complete culture medium under the respective flow conditions. A series of five different flow conditions were investigated, while the overall flow rate was set at 15 μl min^{-1}: (a) ratio central-to-sheath flow 1 : 3 (blue); (b) 1 : 5 (dark green); (c) 1 : 7.5 (light green); (d) 1 : 15 (orange); and (e) 1 : 30 (red). Scale bar: 200 μm.

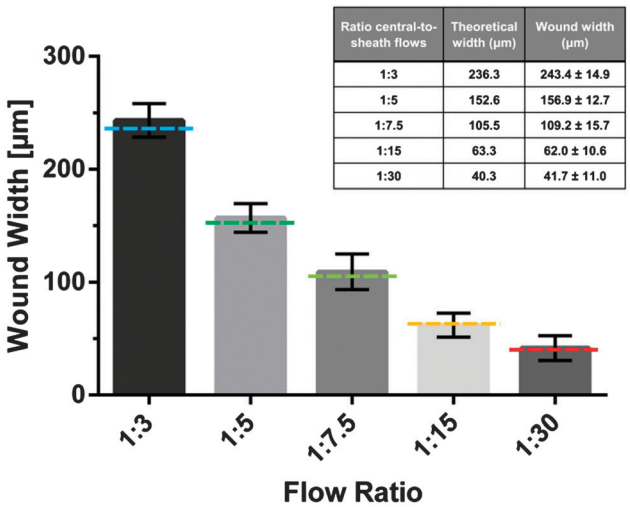

Ratio central-to-sheath flows	Theoretical width (μm)	Wound width (μm)
1:3	236.3	243.4 ± 14.9
1:5	152.6	156.9 ± 12.7
1:7.5	105.5	109.2 ± 15.7
1:15	63.3	62.0 ± 10.6
1:30	40.3	41.7 ± 11.0

Fig. 3 Resulting wound widths after hydrodynamic focusing of 0.5% trypsin–ETDA on a confluent layer of A549 cells, cultured in a 750 μm-wide microchannel. Data represent means ± SD of 4 independent experiments. A series of five different flow conditions were tested. Theoretical wound widths were determined by COMSOL Multiphysics simulations. Theoretical wound widths are displayed as dashed lines with the ratio central-to-sheath flow of 1 : 3 (blue); 1 : 5 (dark green); 1 : 7.5 (light green); 1 : 15 (orange) and 1 : 30 (red).

as shown in Fig. 2. The theoretical values of the central flow widths were obtained by simulating the focused flow using COMSOL Multiphysics. The results confirm both the accuracy and the predictability of the experimental procedure.

The smallest microwounds presented here are 42 μm in width. This correlates with an exposure pattern that only affects three to four neighbouring A549 cells.[36] While wounding, marginal flow fluctuations were observed. These fluctuations are most likely due to technical limitations attributed to the syringe pumps and the deformability of the plastic syringes used for injection. This observation explains the slight differences between the theoretically and experimentally determined wound widths. Furthermore, due to this technical limitation, the formation of microwounds with even smaller dimensions could not be accomplished. Hypothetically, microwounds with dimensions of single cells can be achieved by the use of either higher injection rates or modified channel geometry (Fig. S1, ESI†). For this study, however, the overall flow rate was fixed at 15 μl min^{-1} and only the central-to-sheath flow ratio was altered. Therefore, uniform culture conditions were guaranteed among all flow conditions examined.

Trypsin–ETDA-induced injury: time required for wound creation

Hydrodynamic flow focusing enables targeted and selective cell exposure to various wounding agents or particles. During trypsin–EDTA wounding, cells exposed to the dissociation agents gradually detach from both the neighbouring cells and the underlying substrate. Consequently, affected cells undergo apparent morphologic changes. In the first phase, tight cell–cell contacts get disrupted and the cells start to round up. Following this monolayer disruption, individual cells are progressively detached and ultimately separated from the substrate. In microfluidic wounding, dissociated cells are continuously washed away by the fluid streams, resulting in straight and regular microwounds (Video S1, ESI†). Interestingly, the time needed for the formation of these microwounds strongly differed in the function of the flow ratios (Fig. 4b). The smaller the wound width, the longer it took to create an injury across the whole channel length. To quantify the wound formation over time, time-lapse microscopy of consecutive channel segments was

performed during wounding. The wound formation started at the junction of the three inlet channels with the main channel. From there on, the microwound gradually evolved across the channel. Typically, wider wounds could be generated in only a few minutes, while it took significantly more time to generate smaller wounds. This observation reflects the diffusion phenomena within the system. As previously mentioned, the focused flow of trypsin–EDTA efficiently detaches cells from the substrate. Meanwhile, unexposed cells are protected by the sheath flow consisting of complete culture medium. There is, however, no physical barrier between the cell dissociation agents and the sheath flow. Consequently, diffusive transport occurs within the system. The concentration of dissociation agents is therefore gradually decreasing along the channel length. Lowest concentrations of cell dissociation agents are expected at the very end of the channel. Further, the dissociative activity of trypsin–EDTA is decreased not only due to the diffusion of trypsin–EDTA into the sheathing cell culture medium, but also due to the diffusion of inhibiting molecules from the sheath flow in the opposite direction (*e.g.* Mg^{2+}, Ca^{2+}-ions and trypsin inhibitors). This bi-directional diffusion leads to pronounced gradients in dissociative activity along the channel length. Having a fixed overall flow rate of 15 μl min^{-1} for all experiments, the residence time (t_{res}) and consequently diffusion lengths (L_D) are identical among all flow conditions examined [$L_D = (D \times t_{res})^{1/2}$, with the diffusion coefficient D being constant]. Hence, smaller wounds are proportionally more affected by diffusion phenomena than larger wounds, resulting in longer latency for wound formation.

Trypsin–ETDA-induced injury: control of the wound position

To modify the positioning of the microwounds within the microchannel, complete culture medium was injected at unequal flow rates in the lateral inlets. After convergence at the channel openings, the unequal velocity profiles equilibrated quickly and generated a fully developed parabolic flow profile within tens of micrometers. Thus, the flow of trypsin–EDTA was directed towards the side of the microchannel with the lower sheath flow injection rate. After the formation of the first de-centered microwound, the flow ratio between both sheath flows was reversed, so that the flow of trypsin–EDTA was re-directed towards the opposing side of the microchannel (Fig. 5). A second microwound was formed in the epithelial layer in parallel to the pre-existing one. Since the ratio between wounding and sheath flow was unaffected by this adjustment, both microwounds are of identical widths.

In addition to the tailored wound width, we further demonstrate the predictability and the precision in the wound positioning. In combination with a highly confined trypsin–EDTA exposure, multiple and parallel microwounds within a single epithelial cell layer were achieved (Fig. 5 or Fig. S1, ESI†).

Pepsin–HCl-induced injury: use of physiologically relevant wounding agents

To assess the effect of gastric refluxates on the alveolar epithelium, A549 cells were exposed to a focused flow of acidified pepsin-supplemented serum-free culture medium. In the first set of experiments, the wound creation stopped shortly after the flow convergence at the channel openings (Fig. S2, ESI†). This observation can easily be explained by the rapid diffusion of H^+-ions. In contrast to the aforementioned experiments, the wounding agent features a significant lower pH than the sheath flow (pH 4 *vs.* pH 7.4). In other words, the concentration of H^+-ions in the wounding agent is three orders of magnitude higher than in the sheath flow. Consequently, after convergence at the channel entrance, H^+-ions diffuse from the central wounding to the lateral sheath flows. Due to the high diffusion coefficient of protons ($D_{proton} \approx 2 \times 10^{-9}$ m^2 s^{-1} *vs.* $D_{trypsin} \approx 2.2 \times 10^{-11}$ m^2 s^{-1}), diffusion phenomena are significantly more pronounced in pepsin wounding than in trypsin–EDTA wounding. To overcome this limitation, an aqueous two-phase system was developed with the PEG-rich phase containing the key components of gastric refluxates, HCl and pepsin. Prior to the pepsin dissolution, the wounding phase was pre-acidified to prevent enzyme inactivation at neutral pH-levels. Pepsin was then dissolved to a final concentration of 2.5 mg ml^{-1}, which reflects the highest pepsin concentration

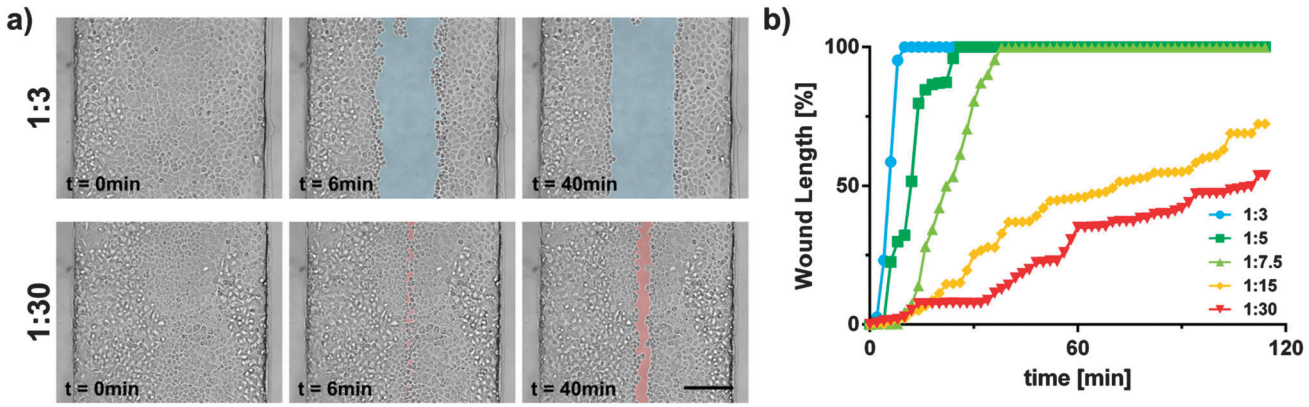

Fig. 4 Wound formation over time. Starting from the channel opening, microwounds gradually evolved across the entire channel length, as monitored by time-lapse microscopy. Representative micrographs (a) are shown for a large wound (top line: ratio central-to-sheath flow 1 : 3) and a small wound (bottom line: 1 : 30). Scale bar: 200 μm. Gradually evolving wound front (b) is shown for a series of decreasing wound widths: 243.4 μm wound (flow ratio 1 : 3; blue ●); 156.9 μm wound (1 : 5; dark green ■); 109.2 μm (1 : 7.5; light green ▲); 62.0 μm (1 : 15; orange ◆); and 41.7 μm (1 : 30; red ▼).

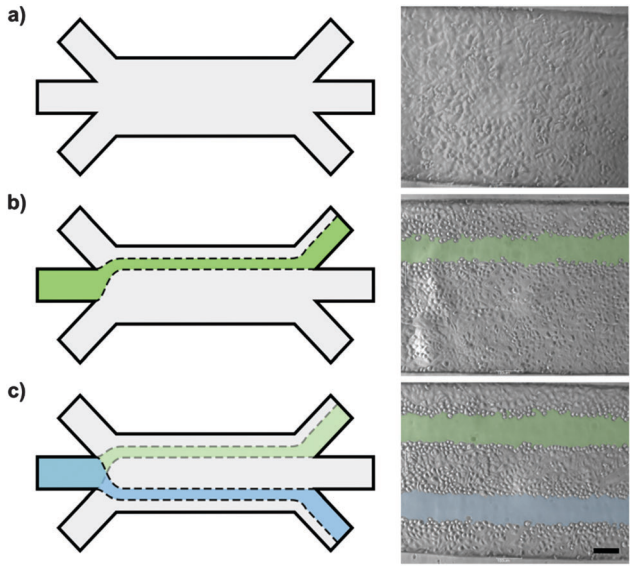

Fig. 5 Parallel microwounds in a 750 μm-wide microchannel. Schematic drawing (a) and micrographs (b) of parallel wounding using a focused flow of 0.5% trypsin–EDTA. Precise control over the injection rates allows for targeted localization of the focused wounding agents within the microchannel. Uneven injection ratios between the two lateral sheath flows were used to de-centralize the focused flow of trypsin–EDTA (green). After formation of the first de-centered 100 μm-wound, the ratio between the lateral sheath flows was reversed, which re-directed the wounding agent towards the opposing channel side (blue), resulting in two uniform and parallel microwounds (c) within a confluent layer of A549 cells. Scale bar: 100 μm.

found in the bronchoalveolar lavage (BAL) fluid of children with GERD.[37] This relatively high value is based on the following two assumptions: (a) gastric refluxates are gradually diluted by mucus and surfactants along the respiratory tract and (b) measurements based on BAL fluids rather reflect the mean concentration levels of the lavaged lung area than local peak values and are likely to underestimate the effective concentrations due to severe dilution by the lavage fluid. It is therefore plausible to assume highest peak concentrations in individual alveoli right after reflux events. In some cases, marginal pH-changes after dissolution of pepsin in pre-acidified medium were observed. Fine titrations were therefore needed for readjusting the ion-concentration to pH 4, which correlates with the threshold value for acidic microaspirations.[11] According to the study of Sweet and colleagues,[9] a significant portion (15%) of reflux events in GERD-positive IPF patients is acidic, irrespective of pre-existing anti-reflux therapy. The modified wounding phase is revealed to remain phase-separated from the sheath flow, which can easily be seen by the clear separation line in Fig. 6 or Fig. S3 (ESI†). This phase-separation is reported along the entire microchannel length. Control experiments with fluorescent tracers, however, revealed that the diffusion between the two-phases was significantly reduced, but not fully prevented by the system (Fig. S4, ESI†). According to Albertsson[38] the exact mechanism at the interface is not well understood and is affected by surface tension properties as well as the densities of the two polymers. Nevertheless, the implementation of an aqueous two-phase system allowed for the formation of pepsin–HCl based microwounds (Fig. 6).

Exposure to the acidified and pepsin-supplemented wounding agent resulted in pronounced epithelial cell retraction and monolayer disruption at the site of exposure. Fig. S5 (ESI†) shows that per se, neither the use of acidic medium nor the addition of pepsin caused similar cell damage. Only in combination with a moderate pH-level, pepsin was revealed to proteolytically cleave cell–cell junctions, leading to the observed cell retraction and monolayer disruption. Interestingly, time-lapse microscopy revealed that the wound formation process underlying pepsin–HCl wounding fundamentally differs from the aforementioned trypsin–ETDA wounding. Whereas trypsin–ETDA exposure induces cleavage of cell anchoring and cell adhesion molecules resulting in cellular release from the substrate (Video S1, ESI†), little to no cell detachment was observed during pepsin–HCl wounding (Video S2, ESI†). This observation is in line with Paradise *et al.*'s findings of integrin $\alpha_v\beta_3$ upregulation upon cellular exposure to acidic pH.[39] Cells exposed to pepsin–HCl tend to actively migrate from the center to the periphery. This hypothesis is further strengthened by the numerous cell protrusions observed at the wound-edging cell border (Fig. 7). Furthermore, affected cells featured slightly condensed cell nuclei. These morphologic changes are indicative of DNA fragmentation during apoptosis. These observations suggest that the microwounds may rather be due to the cellular reaction upon HCl-exposure than the consequence of

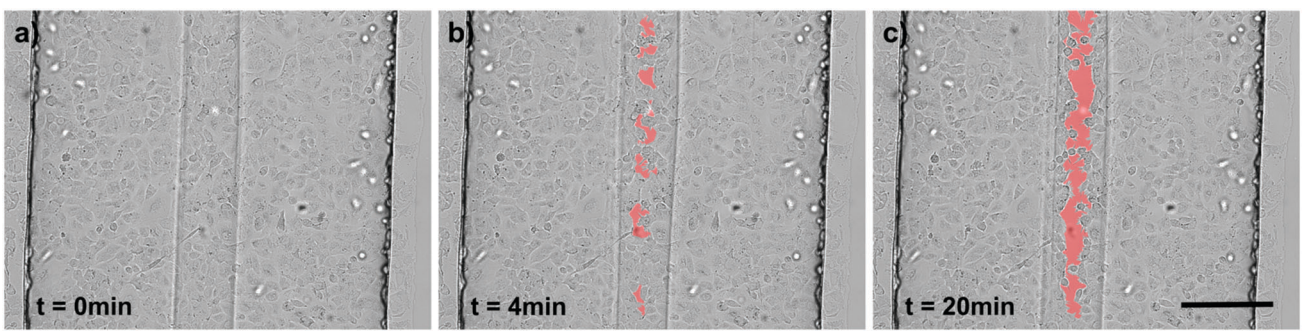

Fig. 6 Time-lapse micrographs during pepsin–HCl-induced wounding of A549 cells cultured in a 750 μm-wide microchannel. A confluent layer of A549 cells (a) was exposed to a focused flow of 2.5 mg ml^{-1} pepsin in pre-acidified serum-free cell culture medium (pH 4). During wounding selective disruption of the monolayer integrity was observed after a short time (b). After long-term exposure a continuous microwound with sharp and distinct wound edges was achieved (c). Scale bar: 200 μm.

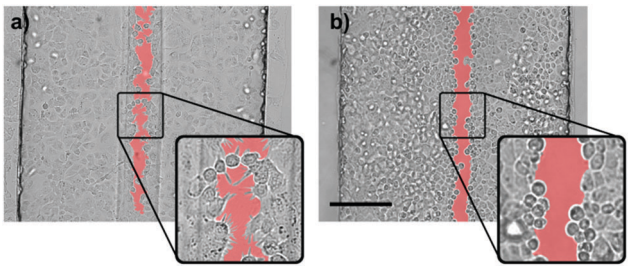

Fig. 7 Micrographs of A549 cells exposed to a focused flow of (a) 2.5 mg ml^{-1} pepsin–HCl and (b) 0.5% trypsin–EDTA. Differences in cell morphology can easily be seen under magnification. Scale bar: 200 μm.

proteolytic cleavage by pepsin (Fig. S5, ESI†). Further investigations are however needed to confirm these observations.

Relevance of proposed wounding model

Idiopathic pulmonary fibrosis is a complex and multi-factorial disease. Formerly, anti-inflammatory therapies have been suggested, but were revealed to be non-effective in IPF. Consequently, to date, therapeutic options remain limited, turning lung transplantation into the last hope for cure in IPF patients. Following these early findings, a new pathomechanism has been suggested. Accordingly, pulmonary fibrosis is the consequence of unregulated wound repair in the alveolus, which may evolve even in the absence of inflammation.[40] Due to its ultrathin epithelium, its large surface area and its exposed site, the human lung is indeed prone to injury. It was therefore the aim of this study to reproduce alveolar wounding by mimicking a hypothetical trigger of IPF, gastric microaspirations. Thereby, we achieved wounds of *in vivo*-relevant dimensions (<200 μm) and with *in vivo*-relevant wounding substances (HCl–pepsin). The chosen concentrations of HCl–pepsin are based on the current literature, but may deviate from concentrations found *in vivo*. The system was developed to recapitulate alveolar wounding in a reproducible manner and is the first step in mimicking the complex and multi-stage pathomechanism underlying IPF. The present system reproduces microaspiration-induced alveolar wounding in a new and unprecedented way and enables wound healing analysis under precisely controlled conditions. We demonstrated HCl–pepsin to synergistically damage alveolar epithelial cells, a finding that directly supports the causal relation between GERD and IPF. Furthermore, HCl–pepsin exposure better portrays the histopathologic finding of apoptotic epithelial cells, as seen in IPF.[41]

Conclusions

Wounding assays have become a valuable and widespread tool for the investigation of cell migration and wound healing. Current wounding systems are often limited in reproducibility and completely fail in modeling wounds with dimensions relevant to the 200 μm wide human alveolus. The formation of such microwounds is, however, of crucial importance for the investigation of chronic lung diseases, such as idiopathic pulmonary fibrosis. It was therefore the objective of this study to create microinjuries of the smallest dimensions with the highest clinical relevance. Thus, possibilities attributed to the recently established microfluidic wounding were explored. The technique was revealed to be robust and highly reproducible. Microwounds of unprecedented dimensions were created and precisely positioned in a microchannel. Further, a multiple of these microinjuries were inflicted in a single epithelial cell layer. Together, it can be concluded that microfluidic wounding allows for tailor-made wounding patterns with unmatched predictability over both the wound width and the wound positioning. With the aid of an aqueous two-phase system, we further demonstrated the versatility of the wounding procedure by using the physiologically more relevant pepsin–HCl wounding agent. Thereby, evidence is provided that episodes of mild acidic exposure disrupt the epithelial barrier integrity, a key event in the development of IPF. This simple wounding lung alveolar model may further help to investigate the complex multi-factorial pathogenesis of IPF.

Acknowledgements

This work was granted by the Swiss National Science Foundation (SNF) and by the Lungenliga Bern. Images were acquired on a device supported by the Microscopy Imaging Center (MIC) of the University of Bern. The authors particularly acknowledge the support and the help from Dr. Fabian Blank from the department of clinical research at the University of Bern. Special thanks goes to Prof. Per-Ake Albertsson for his helpful advice regarding the aqueous two-phase system.

Notes and references

1 N. Kaminski, J. D. Allard, J. F. Pittet, F. Zuo, M. J. Griffiths, D. Morris, X. Huang, D. Sheppard and R. A. Heller, *Proc. Natl. Acad. Sci. U. S. A.*, 2000, **97**, 1778–1783.
2 M. Selman and A. Pardo, *Respir. Res.*, 2002, **8**, 1–8.
3 R. M. Strieter and B. Mehrad, *Chest*, 2009, **136**, 1364–1370.
4 H. Fehrenbach, *Respir. Res.*, 2001, **2**, 33–46.
5 T. J. Desai, D. G. Brownfield and M. A. Krasnow, *Nature*, 2014, **507**, 190–194.
6 J. S. Lee, H. R. Collard, G. Raghu, M. P. Sweet, S. R. Hays, G. M. Campos, J. A. Golden and T. E. King, *Am. J. Med.*, 2010, **123**, 304–311.
7 A. Pacheco-Galván, S. P. Hart and A. H. Morice, *Arch. Bronconeumol.*, 2011, **47**, 195–203.
8 R. W. Tobin, C. E. Pope, C. A. Pellegrini, M. J. Emond, J. Sillery and G. Raghu, *Am. J. Respir. Crit. Care Med.*, 1998, **158**, 1804–1808.
9 M. P. Sweet, M. G. Patti, L. E. Leard, J. A. Golden, S. R. Hays, C. Hoopes and P. R. Theodore, *J. Thorac. Cardiovasc. Surg.*, 2007, **133**, 1078–1084.
10 G. Raghu, T. D. Freudenberger, S. Yang, J. R. Curtis, C. Spada, J. Hayes, J. K. Sillery, C. E. Pope and C. A. Pellegrini, *Eur. Respir. J.*, 2006, **27**, 136–142.
11 D. Sifrim, R. Holloway, J. Silny, Z. Xin, J. Tack, A. Lerut and J. Janssens, *Gastroenterology*, 2001, **120**, 1588–1598.

12 S. Farrell, C. McMaster, D. Gibson, M. D. Shields and W. A. McCallion, *J. Pediatr. Surg.*, 2006, **41**, 289–293.
13 C. Ward, I. A. Forrest, I. A. Brownlee, G. E. Johnson, D. M. Murphy, J. P. Pearson, J. H. Dark and P. A. Corris, *Thorax*, 2005, **60**, 872–874.
14 D. W. Piper and B. H. Fenton, *Gut*, 1965, **6**, 506–508.
15 N. Johnston, P. W. Dettmar, B. Bishwokarma, M. O. Lively and J. A. Koufman, *Laryngoscope*, 2007, **117**, 1036–1039.
16 N. A. Tobey, S. S. Hosseini, C. Caymaz-Bor, H. R. Wyatt, G. S. Orlando and R. C. Orlando, *Am. J. Gastroenterol.*, 2001, **96**, 3062–3070.
17 E. Bathoorn, P. Daly, B. Gaiser, K. Sternad, C. Poland, W. Macnee and E. M. Drost, *Int. J. Inflammation*, 2011, 569416.
18 M. Ochs, J. R. Nyengaard, A. Jung, L. Knudsen, M. Voigt, T. Wahlers, J. Richter and H. J. G. Gundersen, *Am. J. Respir. Crit. Care Med.*, 2004, **169**, 120–124.
19 M. Felder, P. Sallin, L. Barbe, B. Haenni, A. Gazdhar, T. Geiser and O. Guenat, *Lab Chip*, 2012, **12**, 640–646.
20 A. D. van der Meer, K. Vermeul, A. A. Poot, J. Feijen and I. Vermes, *Am. J. Physiol.: Heart Circ. Physiol.*, 2010, **298**, H719–H725.
21 W. Hartwig, J. Werner, R. E. Jimenez, K. Z'graggen, J. Weimann, K. B. Lewandrowski, A. L. Warshaw and C. Fernández-del Castillo, *Am. J. Physiol.*, 1999, **277**, G1008–G1016.
22 D. C. Gotley, A. P. Morgan, D. Ball, R. W. Owen and M. J. Cooper, *Gut*, 1991, **32**, 1093–1099.
23 J. P. Frampton, J. B. White, A. T. Abraham and S. Takayama, *J. Visualized Exp.*, 2013, 16–20.
24 C. Bathany, J. Park, Y.-K. Cho and S. Takayama, *J. Mater. Chem. B*, 2013, **1**, 6020.
25 D. Petrak, E. Atefi, L. Yin, W. Chilian and H. Tavana, *Biotechnol. Bioeng.*, 2013, **111**, 404–412.
26 J. C. McDonald and G. M. Whitesides, *Acc. Chem. Res.*, 2002, **35**, 491–499.
27 M. W. Toepke and D. J. Beebe, *Lab Chip*, 2006, **6**, 1484–1486.
28 E. Planus, S. Galiacy, M. Matthay, V. Laurent, J. Gavrilovic, G. Murphy, C. Clérici, D. Isabey, C. Lafuma and M. P. D'Ortho, *J. Cell Sci.*, 1999, **112**, 243–252.
29 T. Geiser, K. Atabai, P.-H. Jarreau, L. B. Ware, J. Pugin and M. A. Matthay, *Am. J. Respir. Crit. Care Med.*, 2001, **163**, 1384–1388.
30 V. K. Sidhaye, K. S. Schweitzer, M. J. Caterina, L. Shimoda and L. S. King, *Proc. Natl. Acad. Sci. U. S. A.*, 2008, **105**, 3345–3350.
31 D. J. Tschumperlin, J. Oswari and S. S. Margulies, *Am. J. Respir. Crit. Care Med.*, 2000, **162**, 357–362.
32 N. J. Douville, P. Zamankhan, Y.-C. Tung, R. Li, B. L. Vaughan, C.-F. Tai, J. White, P. J. Christensen, J. B. Grotberg and S. Takayama, *Lab Chip*, 2011, **11**, 609–619.
33 S. Hammerschmidt, H. Kuhn, T. Grasenack, C. Gessner and H. Wirtz, *Am. J. Respir. Cell Mol. Biol.*, 2004, **30**, 396–402.
34 L. M. Crosby, C. Luellen, Z. Zhang, L. L. Tague, S. E. Sinclair and C. M. Waters, *Am. J. Physiol.: Lung Cell. Mol. Physiol.*, 2011, **301**, L536–L546.
35 G. Raghu and K. C. Meyer, *Eur. Respir. J.*, 2012, **39**, 242–245.
36 R. Jiang, H. Shen and Y.-J. Piao, *Rom. J. Morphol. Embryol.*, 2010, **51**, 663–667.
37 V. Starosta, R. Kitz, D. Hartl, V. Marcos, D. Reinhardt and M. Griese, *Chest*, 2007, **132**, 1557–1564.
38 P.-A. Albertsson, *Partition of Cell Particles and Macromolecules*, 1971.
39 R. K. Paradise, D. a Lauffenburger and K. J. Van Vliet, *PLoS One*, 2011, **6**, e15746.
40 M. Selman, T. E. King and A. Pard, *Ann. Intern. Med.*, 2001, **134**, 136–151.
41 J. V. Barbas-Filho, M. A. Ferreira, A. Sesso, R. A. Kairalla, C. R. Carvalho and V. L. Capelozzi, *J. Clin. Pathol.*, 2001, **54**, 132–138.

